

Synthesis of High Coercivity Cobalt Nanotubes with Acetate Precursors and Elucidation of the Mechanism of Growth

T. N. Narayanan,[†] M. M. Shaijumon,[‡] P. M. Ajayan,^{*,‡} and M. R. Anantharaman^{*,†}

Department of Physics, Cochin University of Science & Technology, Cochin-22, Kerala, India, and Department of Mechanical Engineering & Materials Science, Rice University, Houston, Texas 77005

Received: April 22, 2008; Revised Manuscript Received: July 3, 2008

Cobalt nanotubes (CoNTs) with very high longitudinal coercivity were prepared by electrodeposition of cobalt acetate for the first time by using anodized alumina (AAO) template. They were then characterized with X-ray diffraction (XRD), a field emission scanning electron microscope (FESEM), and a transmission electron microscope (TEM). Formation of a highly ordered hexagonal cobalt phase is observed. Room temperature SQUID (superconducting quantum interference device) magnetometer measurements indicate that the easy axis of magnetization is parallel to the nanotube axis. These CoNTs exhibit very high longitudinal coercivity of ~ 820 Oe. A very high intertubular interaction resulting from magnetostatic dipolar interaction between nanotubes is observed. Thick-walled nanotubes were also fabricated by using cobalt acetate tetrahydrate precursors. A plausible mechanism for the formation of CoNTs based on mobility assisted growth is proposed. The role of the hydration layer and the mobility of metal ions are elucidated in the case of the growth mechanism of one-dimensional geometry.

Introduction

Design and control of nanowire and nanotube growth with a limited degree of complexity will surely impact the development of nanotechnology.¹ Soon after the discovery of carbon nanotubes by Iijima,² nanotube-based materials received significant attention from the scientific community because of their extensive application potential in nanodevices and sensors.³ Nanohole arrays having uniform size and shape have been identified as potential materials for fabricating various functional nanodevices.^{4–7} Tubular structures offer multitudes of opportunities because they can be used as pipes, microcavities, or microcapsules. Nanoholes, for example, with large surface area, can successfully replace the low-purity nanoparticles that are prepared by using more sophisticated techniques for various applications such as catalysis, sensor technology, high-density magnetic storage, and delivery vehicles.^{8,9} Inorganic nanotubes have also attained considerable attention during the past few years due to their diverse utilities in racemic mixtures, sensors, selective separation, or selective ion transportation.⁸ However, literature on noncarbon nanotubes is limited as compared to their carbon counterparts.^{10–14} Among the non-carbon cousins, much interest has been devoted to metal nanotubes and nanowires. Several techniques are reported for the synthesis of metal nanotubes. These include chemical routes such as chemical reduction of metallic complexes and chemical vapor infiltration within porous templates such as AAO or polymer nanochannels.^{4,9,10,15} There are also reports where nanotubes and nanowires have been synthesized by using highly sophisticated techniques such as pulse laser deposition or molecular beam epitaxy.^{16,17}

Ferromagnetic nanotubes based on Ni, Fe, and Co are being investigated in great detail due to their application potential in

diverse fields such as perpendicular magnetic recording, cell separation, diagnosis, therapeutics, and magnetic resonance imaging for detection. The ease with which they can be functionalized by using a specific group is an added advantage of these nanostructures and can be used for drug targeting and other applications in biotechnology.^{18,19} However, not much literature exists regarding the utilization of magnetic nanotubes in medicine. A survey of the literature reveals that a systematic method of preparation of nanotubes and elucidation of growth mechanism is largely elusive.^{3,20}

Electrodeposition over a nanoporous membrane is a simple, low-cost, and ingenious technique for the preparation of one-dimensional structure with high purity. The ability of this technique to tune the material properties by controlling the length and diameter makes it promising for nanoscale material fabrication as an alternative to more expensive techniques such as molecular beam epitaxy and microlithography.²¹

Most of the reports on the synthesis of magnetic nanotubes are by chemical modification of inner surface of the porous template prior to the deposition.^{4,9,10,15,17} However, these techniques result in low yield and impure structures. Moreover, the mechanism leading to the formation of nanostructures from nanoporous template is seldom elucidated, which is very essential for tailoring the properties of these nanostructures.³

In this paper, we report the synthesis of thin-walled and thick-walled cobalt nanotubes using cobalt acetate and cobalt acetate tetrahydrate precursors, respectively. A plausible mechanism for the formation of CoNTs will be elucidated and the role of metal ion and hydration layer will be examined in the case of one-dimensional geometry.

Experimental Section

Alumina membranes (Whatman) of high purity and uniform pore density, with an average pore diameter ~ 150 nm and thickness ~ 60 μm , were employed for electrodeposition. Initially, a layer of Ag (about 200 nm thick) was thermally

* Corresponding authors. E-mail: mraiayer@yahoo.com and ajayan@rice.edu.

[†] Cochin University of Science & Technology.

[‡] Rice University.

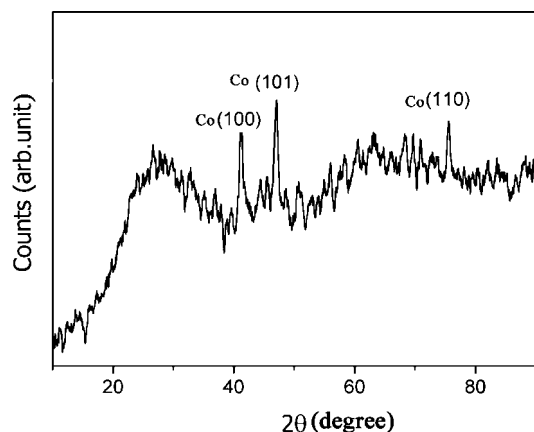


Figure 1. XRD pattern of cobalt nanotubes with alumina template.

evaporated onto one side of the AAO template, which acted as the working electrode for the electrochemical deposition. The electrodeposition was carried out on the nanopores, using a standard three-electrode potentiostat system (Princeton EG&G 273 A). Ag/AgCl was the reference electrode and platinum was used as the counter electrode. It is noteworthy that by using this process the length of the metal nanotube can be controlled by varying the time of deposition. Cobalt acetate (0.2 M) was used as the precursor for electrodeposition. Once the electrodeposition was over, AAO was dissolved with 3 M sodium hydroxide (NaOH). An X-ray powder diffraction pattern of nanotubes was recorded with Cu K α radiation, $\lambda = 1.5418\text{\AA}$ (Rigaku Dmax-C). The morphology of the nanotubes after removing the template was studied with a field emission scanning electron microscope (SEM), JSM-6335 FESEM. Room temperature and low temperature magnetic properties of these nanotubes were investigated by using a SQUID magnetometer (MPMS-5S XL Quantum Design). Transmission electron microscopy (TEM) experiments were performed with a JEM 2010 transmission electron microscope.

Results and Discussion

The X-ray diffraction (Rigaku Dmax-C) pattern (Figure 1) of cobalt nanotubes indicates the formation of the polycrystalline pure cobalt hexagonal close packed phase (space group: $p63/mmc$). Broad features appearing in the $15\text{--}35^\circ$ 2θ range arise from the amorphous alumina. This is in agreement with earlier reports.³

The FESEM images of cobalt nanotubes, after removal of supporting alumina template by alkaline treatment, are depicted in Figure 2. Figure 3a shows the TEM image of cobalt nanotubes, and Figure 3b, the energy dispersive spectrum (EDS) of cobalt nanotubes, confirms the presence of cobalt in cobalt nanotubes and also establishes the absence of other elemental impurities (for details, see the Supporting Information, Figures S1 and S2).

Magnetisation Studies. Magnetic hysteresis loops, which display the magnetic response of a magnetic sample to an external applied magnetic field, have been used to characterize the nanostructured materials. Room temperature $M(H)$ behaviors for both fields parallel and perpendicular to the tube studied by using a SQUID magnetometer are shown in Figure 4. Magnetisation measurements were carried out by keeping the nanotubes inside the pores of alumina in order to keep the alignment of tubes.

Figure 4b shows that for a field parallel to the tube the coercivity $H_c = 824$ Oe and for the perpendicular field H_c is

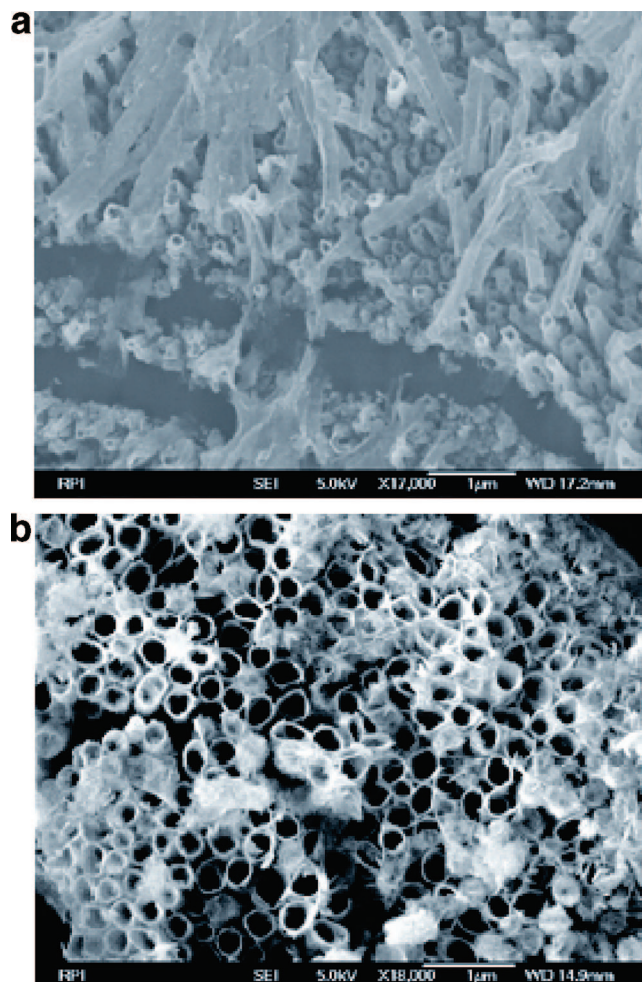


Figure 2. FESEM images of cobalt nanotubes: (a) 1 h electrodeposition and (b) top view of the 5 h deposited nanotube.

123 Oe. This very high coercivity observed for the field parallel to the tube (highest reported value for cobalt wire system of the same diameter, ~ 150 nm)^{10,19,21,22} indicates that easy axis of magnetization is parallel to the tube axis. Perfect ordering and defect free end surfaces may be the reasons for the exhibition of high coercivity in these one-dimensional structures. Recent studies indicate that parameters like shape, wire ends, and diameter fluctuations will lead to localized magnetization reversal, resulting in reduction of coercivity.²³ Even though the magnetization is parallel to the tube, squareness (M_r/M_s) is less compared to the M_r/M_s value obtained with the field perpendicular to the tube and hence a higher anisotropy results along the tube. This is due to the high intertubular interaction where the intertubular separation is ~ 100 nm. Since alumina template is not able to mediate exchange interactions over more than a few interatomic distances, the interactions between the tubes are predominantly magnetostatic dipole interactions.²⁴ The magnetic field produced by a dipole at a distance x in a direction perpendicular to the dipole is given by the relation

$$H_x = \frac{m}{\left(x^2 - \frac{l^2}{4}\right)^{3/2}} \quad (1)$$

where m is the magnetic moment and l is the length of the dipole. So this field effectively acts as the demagnetizing field and will become an important factor when the intertubular distance is of the same order of tubular diameter. The magne-

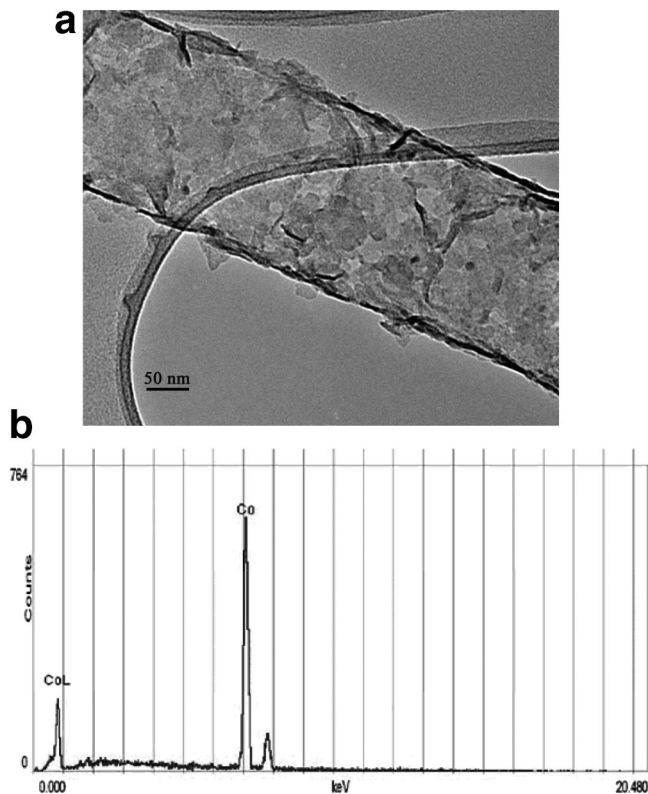


Figure 3. (a) TEM image and (b) EDS of the cobalt nanotube.

tostatic interaction between larger nanometer tubes or wires, which are closely packed in an alumina template, is more important than that between smaller ones.²⁵ The main effect of wire or tube interaction is to decrease the saturation field for perpendicular fields,²⁶ and this effectively reduces the anisotropy. Figure 5 shows the $M-H$ behavior of cobalt nanotubes for the field perpendicular to the tube.

The enhancement of H_c at low temperature ($H_c \approx 345$ Oe) is consistent with the monotonic increase of uniaxial anisotropy constant with decreasing temperature, with the basic assumption that the shape anisotropy is independent of temperature for high aspect ratio tubes.²²

Thick-Walled Cobalt Nanotubes and Growth Mechanism.

Thick-walled nanotubes (some of them are completely filled as wires) of cobalt nanotubes were produced (for details, see the Supporting Information, Figure S3) when the precursor was replaced by an aqueous solution of cobalt acetate tetrahydrate. Parameters like pH, molarity and field gradient are kept constant for both depositions (cobalt acetate and cobalt acetate tetrahydrate). Figure 6.a. and 6.b. show the FESEM images (side view and top view) of thick-walled cobalt nanotubes and Figure 6c. depicts the TEM photograph of thick walled nanotube.

Understanding the growth mechanism plays an important role in the controlling and designing nanostructures. Yao et al.²⁷ have explained a possible growth mechanism for the formation of metal nanostructures over alumina based on a current assisted growth mechanism. However, the role of metal ion mobility was not forthcoming in their investigations. It must be noted here that Yao et al. have carried out the electrodeposition at constant current density while the present set of experiments was carried out by keeping the voltage constant.

A possible mechanism based on the mobility assisted formation of nanotubes and wires in the case of constant voltage (potentiostatic) deposition is discussed below. It is an already established fact that the growth mechanism in a porous material originates

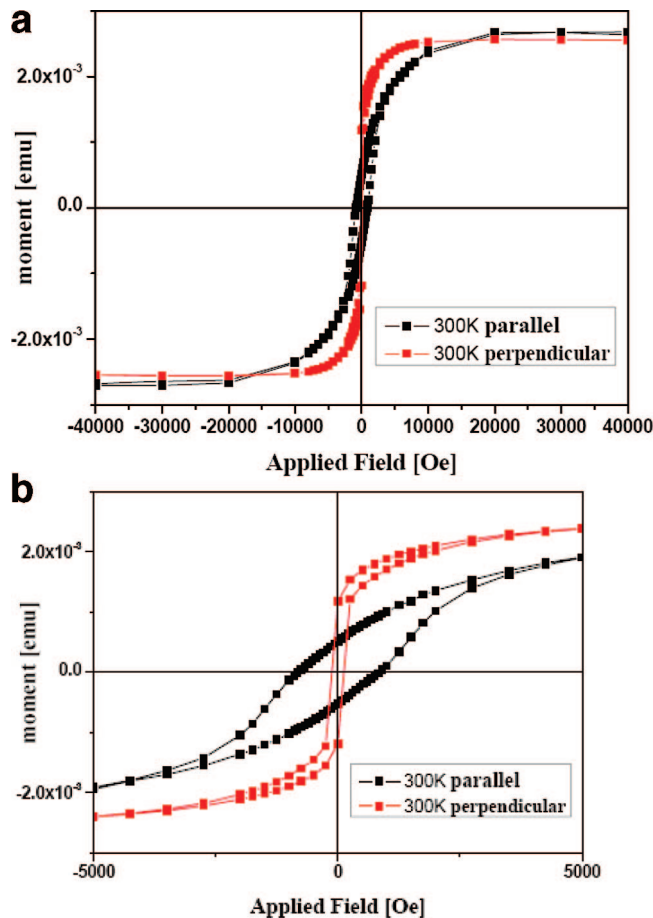


Figure 4. (a and b) Room temperature $M-H$ curve for Co nanotubes.

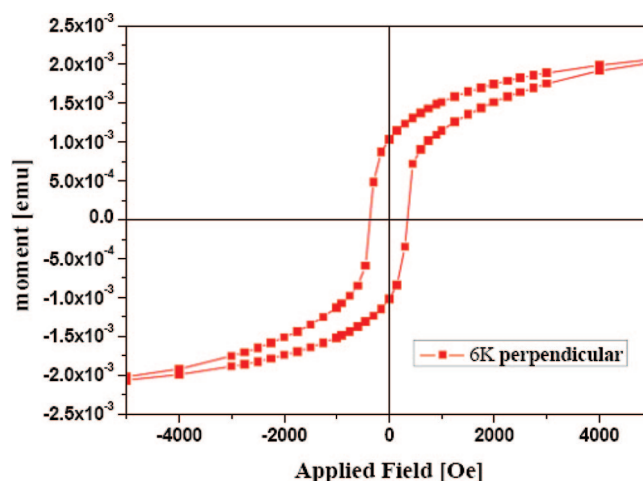
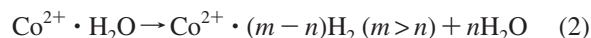


Figure 5. $M-H$ curve for the field perpendicular to the tube at 6 K.

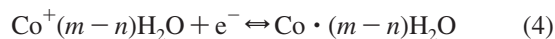
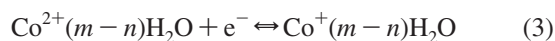
from the cathode surface at the bottom edge of the pore. Because of their reduced coordination number and high surface area, porous parts of the template (alumina) serve as energetically favorable sites for initiating metal atom adsorption.^{28,29}

When a negative potential is applied to the working electrode, divalent metal ions of Co^{2+} surrounded by the hydration layer move toward the cathode and reduce to metal. This is a tristage process as follows:

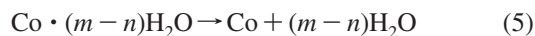
1. The hydration number of metal ions decreases and the metal ions (Co^{2+}) are rearranged in solution near the cathode surface, which can be written as follows



2. Co^{2+} ions, surrounded by water molecules are then reduced. This is a step-by-step process as observed in eqs 3 and 4,



3. The final step is an adsorption process and the adsorbed metal cobalt discards the hydration layer and enters into the crystal lattice and is represented by eq 5.



The movement rate of ions in a given electric field E depends on two factors, the mobility of the ions and the potential gradient across the working and counter electrode.

$$V_+ = \mu_+ \frac{dE}{dx} \quad (6)$$

$$V_- = \mu_- \frac{dE}{dx} \quad (7)$$

where V_+ , V_- are the movement rates of cobalt ion and acetate ion and μ_+ , μ_- are the mobility of cobalt ion and acetate ion, respectively. The components of the metal ion movement rate V_{\parallel} and V_{\perp} and their competitions are the key parameters determining the resultant geometry after electrodeposition. Cao et al.³ reported the formation of nanowires under low applied current density, where in $V_{\parallel} \approx V_{\perp}$. At high applied current densities, this will lead to high values of dE/dx , and nanotubes are the resultant geometries because in this case $V_{\parallel} \gg V_{\perp}$. In our investigation a constant potential is maintained (potentiostatically) for electrodeposition instead of keeping the current density constant (galvanostatically). A schematic representation of the mobility assisted growth of nanotubes and wires is depicted in Figure 7, parts a and b, respectively. It is to be noted here that the mobility of cobalt ions in cobalt acetate and cobalt acetate tetrahydrate is different. It is a well-known fact from basic electrochemistry that the extra hydration in tetrahydrate will act as a dead layer and shield the metal ions from an external potential. Hence, the mobility of metal ions capped with this hydrated layer is effectively reduced. This case is similar to that of low current density deposition in current directed tubular growth mechanism (CDTG) as discussed by Yao et al., where V_{\parallel} is similar to V_{\perp} . Here, as the time increases, metal atoms will fill most of the template pores until they are completely filled. But in the case of cobalt acetate, cobalt ion mobility will be much higher and also have an enhanced parallel velocity component. So a Co nanotube is the resulting one. The key factors determining the morphology of the one-dimensional objects (nanowires or tubes) in an electrodeposition are the mobility of metal ions and number of hydrated ions attached. This mechanism is validated and generalized by other precursors like cobalt sulfate too. This can be treated as a general growth mechanism in the constant voltage deposition process for all types of metal nanowires, and open the possibility for controlling the formation of one-dimensional structures. Optimization and standardization of process parameters will help to control the thickness of nanotubes and thereby pave way for tailoring the properties.

Conclusion

Cobalt nanotubes of highly ordered and hexagonal close packed structure are formed by the electrodeposition of cobalt acetate for the first time in a constant potential of -1 V. These

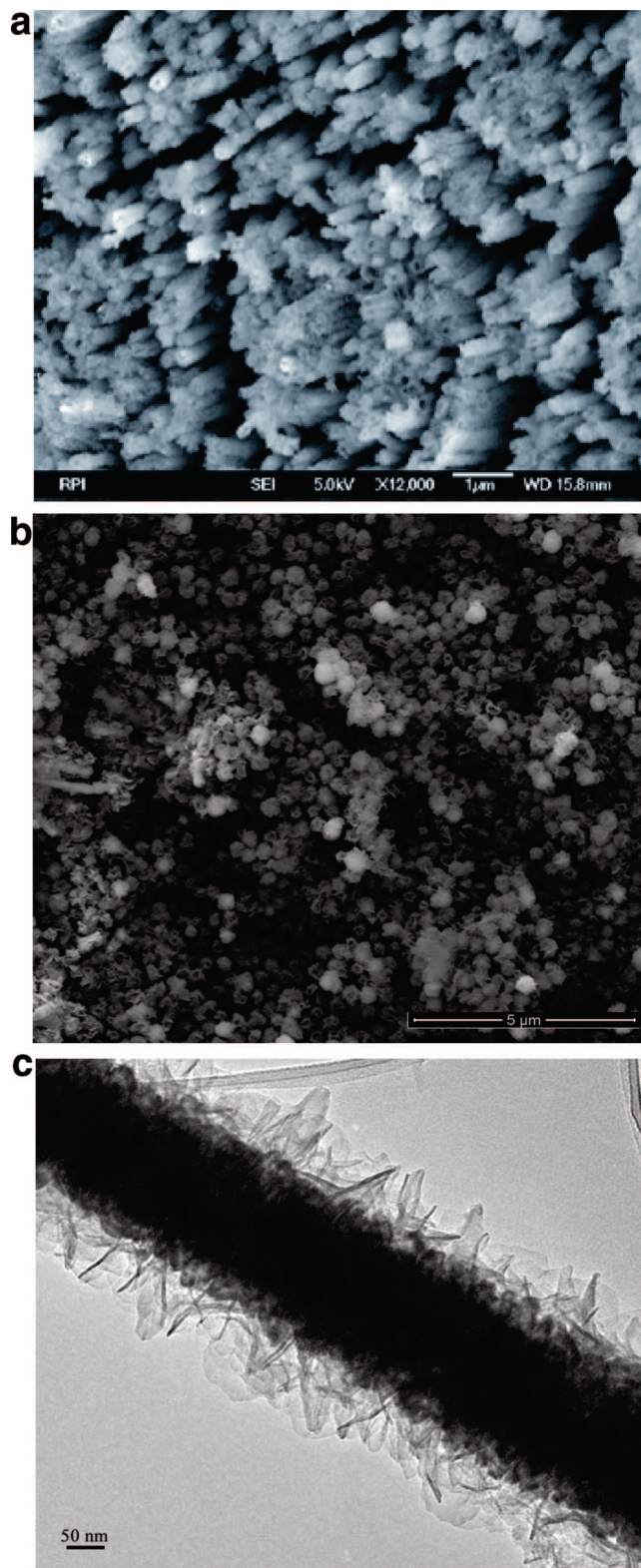


Figure 6. (a and b) FESEM images and (c) TEM image of thick-walled cobalt nanotubes.

nanotubes have a maximum outer diameter of ~ 150 nm and length of $\sim 50 \mu\text{m}$ for 5 h electrodeposition. They exhibit the highest reported longitudinal coercivity of ~ 820 Oe at room temperature. They exhibit a low anisotropy along the tube axis compared to the direction perpendicular to the tube. This reduction in anisotropy and thereby saturating field perpendicular to the tube axis is explained as due to the high magnetostatic dipolar interaction between nanotubes packed very closely in

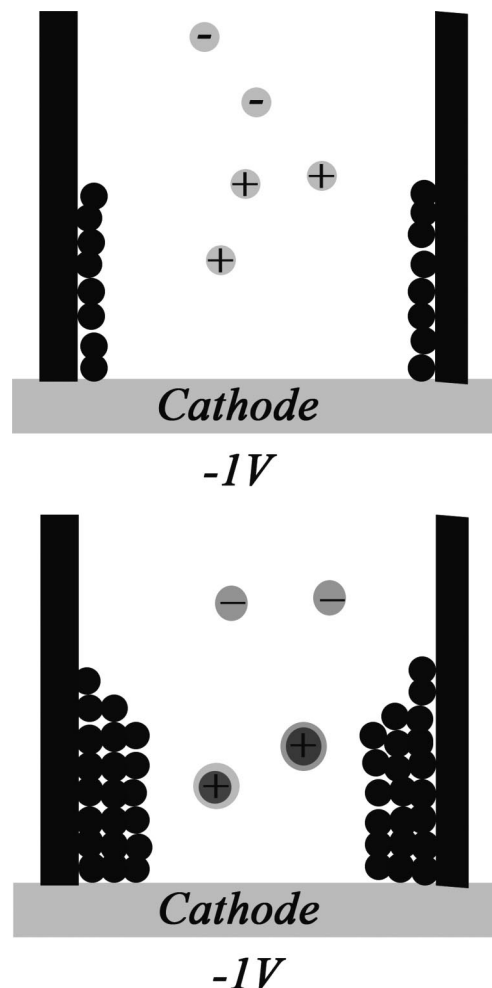


Figure 7. Schematic diagram showing the growth mechanism (at a particular instant of growth) of cobalt nanotubes with two precursors: (a) cobalt acetate and (b) cobalt acetate tetrahydrate. A shell of extra hydration layer on the metal ion is shown in panel b.

the alumina membrane. These nanotubes with very high coercivity are promising for high-density data storage and other applications. Cobalt acetate tetrahydrate is employed to fabricate thick-walled nanotubes. A plausible mechanism for the formation of nanotubes based on the mobility assisted growth mechanism is elucidated on the basis of a modified model. Such tunability and control over the formation of magnetic nanotubes or wire opens a unique opportunity to systematically approach these one-dimensional structures for exploring their possible applications in areas such as magnetic recording, sensors, catalysis, and so forth.

Acknowledgment. T.N.N. acknowledges the financial support received from the Interconnect Focus Center at Rensselaer Polytechnic Institute, Troy, New York. T.N.N. thanks Kerala State Council for Science, Technology and Environment (D.O. No. 004/FSHIP/05/KSCSTE), Kerala, India, for financial support

in the form of a fellowship. T.N.N. and M.R.A. acknowledge Prof. Gunter Schatz, Prof. Manfred Albrecht, and Dr. Ildico Guhr, Department of Physics, University of Konstanz, for SQUID measurements and fruitful discussions. M.R.A. thanks DST-DAAD PPP for awarding an exchange program.

Supporting Information Available: FT IR spectrum and micro-Raman studies of cobalt nanotubes, after the etching of the AAO template with 3 M NaOH, in order to elucidate the purity of cobalt nanotube, and an energy dispersive spectrum of thick-walled cobalt nanotubes. This material is available free of charge via the Internet at <http://pubs.acs.org>.

References and Notes

- (1) Meng, G. W.; Jung, Y. J.; Cao, A.; Vajtaj, R.; Ajayan, P. M. *PNAS* **2005**, *102*, 7074.
- (2) Lijima, S. *Nature* **1991**, *354*, 56.
- (3) Cao, H.; Wang, L.; Qiu, Y.; Wu, Q.; Wang, G.; Zhang, L.; Liu, X. *ChemPhysChem* **2006**, *7*, 1500.
- (4) Yanagishita, T.; Nishio, K.; Masuda, H. *Adv. Mater.* **2005**, *17*, 2241.
- (5) Park, M.; Harrison, C.; Chaikin, P. M.; Register, R. A.; Adamson, D. H. *Science* **1997**, *276*, 1401.
- (6) Tonucci, R. J.; Justus, B. L.; Campillo, A. J.; Ford, C. E. *Science* **1992**, *258*, 783.
- (7) Whitney, T. M.; Jiang, J. S.; Searson, P. C.; Chien, C. L. *Science* **1993**, *261*, 1316.
- (8) Steinhart, M.; Wehrspohn, R. B.; Gosele, U.; Wendorff, J. H. *Angew. Chem., Int. Ed.* **2004**, *43*, 1334.
- (9) Bao, J.; Tie, C.; Xu, Z.; Zhou, Q.; Shen, D.; Ma, Q. *Adv. Mater.* **2001**, *13*, 21.
- (10) Nielsch, K.; Castano, F. J.; Matthias, S.; Lee, W.; Ross, C. A. *Adv. Eng. Mater.* **2005**, *7*, 4.
- (11) Xia, Y.; Yang, P.; Sun, Y.; Wu, Y.; Mayers, B.; Gates, B.; Yin, Y.; Kim, F.; Yan, H. *Adv. Mater.* **2003**, *15*, 353.
- (12) Rao, C. N. R.; Nazh, M. *Dalton Trans.* **2003**, *1*, 1.
- (13) Remskar, M. *Adv. Mater.* **2004**, *16*, 1497.
- (14) Tenne, R. *Colloids Surf., A* **2002**, *208*, 83.
- (15) Lee, W.; Scholz, R.; Nielsch, K.; Gosele, U. *Angew. Chem., Int. Ed.* **2005**, *44*, 6050.
- (16) Heydon, G. P.; Hoon, S. R.; Farley, A. N.; Tomlinson, S. L.; Valera, M. S.; Attenborough, K.; Schwarzacher, W. *J. Phys. D: Appl. Phys.* **1997**, *30*, 1083.
- (17) Sharif, R.; Shamaila, S.; Ma, M.; Yao, L. D.; Yu, R. C.; Han, X. F.; Khaleeq-ur-Rahman, M. *Appl. Phys. Lett.* **2008**, *92*, 032505.
- (18) Bao, J.; Chen, W.; Liu, T.; Zhu, Y.; Jin, P.; Wang, L.; Liu, J.; Wei, Y.; Li, Y. *ACS Nano* **2007**, *1*, 293.
- (19) Srivastava, A. K.; Singh, R. S.; Sampson, K. E.; Singh, V. P.; Ramanujan, R. V. *Metall. Mater. Trans. A* **2007**, *38A*, 717.
- (20) Wang, T.; Wang, Y.; Li, F.; Xu, C.; Zhou, D. *J. Phys.: Condens. Matter* **2006**, *18*, 10545.
- (21) Fert, A.; Piroux, L. *J. Magn. Magn. Mater.* **1999**, *200*, 338.
- (22) Henry, Y.; Ounadjela, K.; Piroux, L.; Dubois, S.; George, J. M.; Duvail, *Eur. Phys. J. B* **2001**, *20*, 35.
- (23) Yu, C. Y.; Yu, Y. L.; Sun, H. Y.; Xu, T.; Li, X. H.; Li, W.; Gao, Z. S.; Zhang, X. Y. *Mater. Lett.* **2007**, *61*, 1859.
- (24) Sellmyer, D. J.; Zheng, M.; Skomski, R. *J. Phys.: Condens. Matter* **2001**, *13*, R433.
- (25) Sun, L.; Hao, Y.; Chein, C. L.; Searson, P. C. *IBM J. Res. Dev.* **2005**, *49*, 1.
- (26) Martin, J. I.; Noguees, J.; Liu, K.; Vicent, J. L.; Schuller, I. K. J. *Magn. Mater.* **2003**, *256*, 449.
- (27) Yoo, W. C.; Lee, J. K. *Adv. Mater.* **2004**, *16*, 1097.
- (28) Lahav, M.; Sehayek, T.; Vaskevich, A.; Rubinstein, I. *Angew. Chem.* **2003**, *115*, 5734.
- (29) Lahav, M.; Sehayek, T.; Vaskevich, A.; Rubinstein, I. *Angew. Chem., Int. Ed.* **2003**, *42*, 5576.